Supporting Information for

Predicting the Macroscopic Fracture Energy of Epoxy Resins from Atomistic Molecular Simulations

Zhaoxu Meng[1], M. A. Bessa[2], Wenjie Xia[1], Wing Kam Liu[2] and Sinan Keten[1, 2]*

[1] Department of Civil and Environmental Engineering, Northwestern University, 2145 Sheridan Road, Evanston, IL 60208-3111, United States

[2] Department of Mechanical Engineering, Northwestern University, 2145 Sheridan Road, Evanston, IL 60208-3111, United States

* Corresponding authors: s-keten@northwestern.edu

1. Details of the tensile deformation

1.1. Potential energy evolution

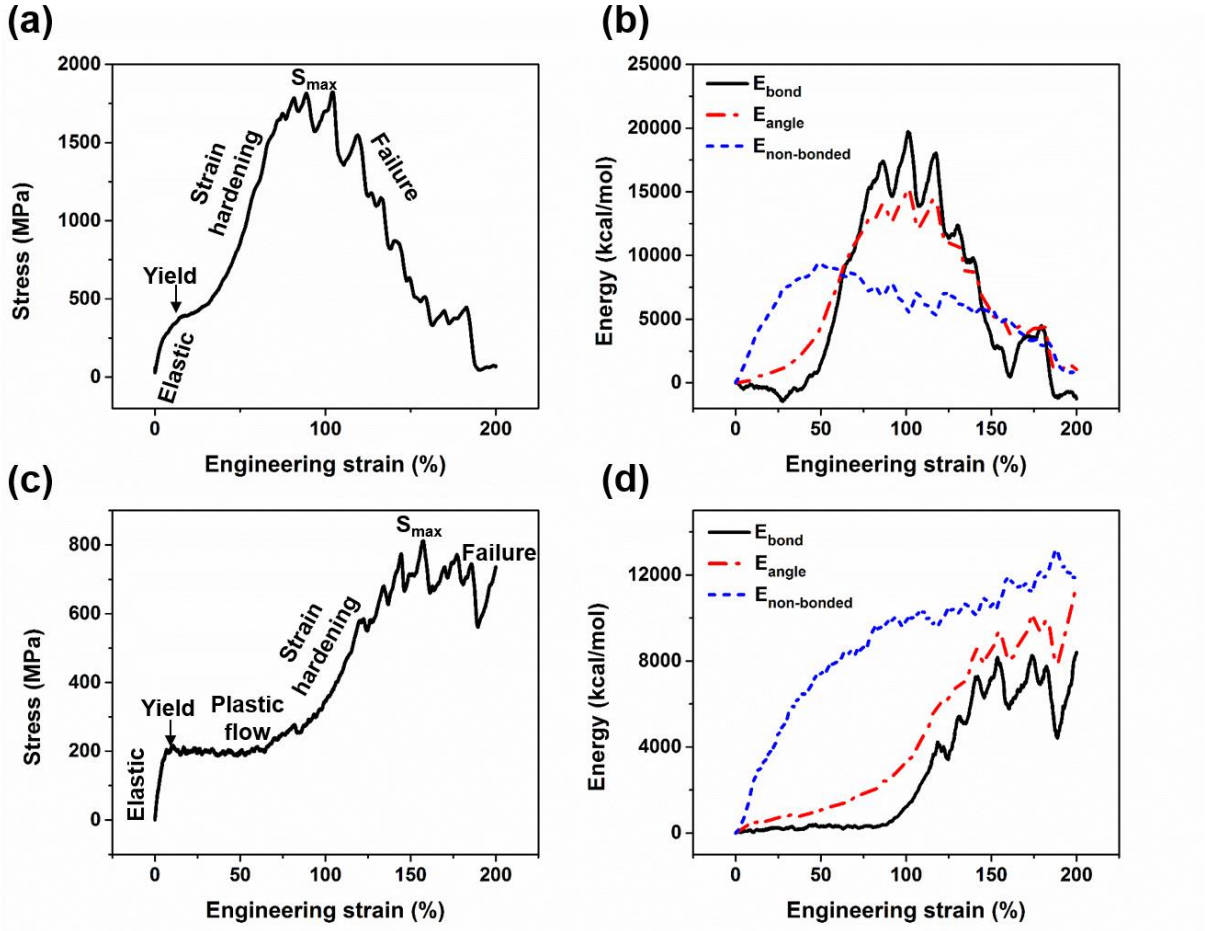

Figure S1. (a) Stress vs. strain curve for epoxy 3501-6. (b) Potential energy evolution during deformation for epoxy 3501-6. (c) Stress vs. strain curve for epoxy Epon 825. (d) Potential energy evolution during deformation for epoxy Epon 825.

To quantify the structural changes during uniaxial tension of the two representative epoxy resins studied herein, we decompose the total potential energy into sub-categories and relate the potential energy to multiple stages in the stress vs. strain curves such as elastic response, yield/plastic flow, hardening, maximum stress and ultimate failure. In Fig. S1(b) and (d), we find that the energy from non-bonded interactions, including both van der Waals and Coulombic interactions, increases with strain more obviously in the small deformation, while the bond

energy stays almost constant before strain hardening, which indicates that bond stretching contributions are not significant. After yielding, the angle energy starts to increase due to chain alignment and reorientation under the constraints of crosslinks. During the hardening stage, chain extension becomes more substantial, and the potential energy increase from contributions of the bond and angle becomes dominant compared to non-bonded interactions. In the final maximum stress and failure stage where stress oscillates dramatically, the bond and angle energies undergo large oscillations, indicating that covalent bonds are breaking due to chain scission. It should be noted the non-bonded energy in the 3501-6 case starts to decrease after reaching the failure stage, which can be explained by the local relaxation after chain breaking.

By comparing the potential energy evolutions for the two representative epoxy resins, it is clear that for the Epon 825 case, the bond energy starts to increase at a larger strain but in a less abrupt manner, indicating that more chain rearrangement events could occur during deformation due to lower crosslink density. This characteristic difference between two epoxies may also explain the molecular origin of the higher fracture energy observed for Epon 825.

1.2. Conformational change during deformation

To quantitatively describe the conformations, we use end-to-end chain length distribution of monomers in the crosslinked structure to describe the extension of the molecular segments (illustrated in Fig. S2(a)). For the reorientation of the segments, we calculate the angle between chain orientation and loading direction, and then use Herman's order parameter $f = \frac{1}{2} < 3cos^2\theta - 1 >$ to describe the process,[1] with higher values indicating more monomers orienting orderly towards loading direction.

The results show that the segments are not effectively stretched before the strain reaches 30%, corresponding to the regime where bond energy does not increase preceding the onset of strain hardening. At a strain of 80%, the segments start to exhibit significant elongation as shown in Fig. S2(b), corresponding to a substantial increase in bond potential energy. Fig. S2(c) shows the reorientation process of segments during deformation. There is already observable reorientation happening in the system at 30% strain, indicated by the steady increase of the order parameter. This reorientation process corresponds to the increase of angle potential energy before the strain

hardening regime. Finally, at a strain of 80%, segments reach the reorientation limit brought by the crosslinks and the order parameter no longer increases. These conformation changes correlate well with the potential energy evolution.

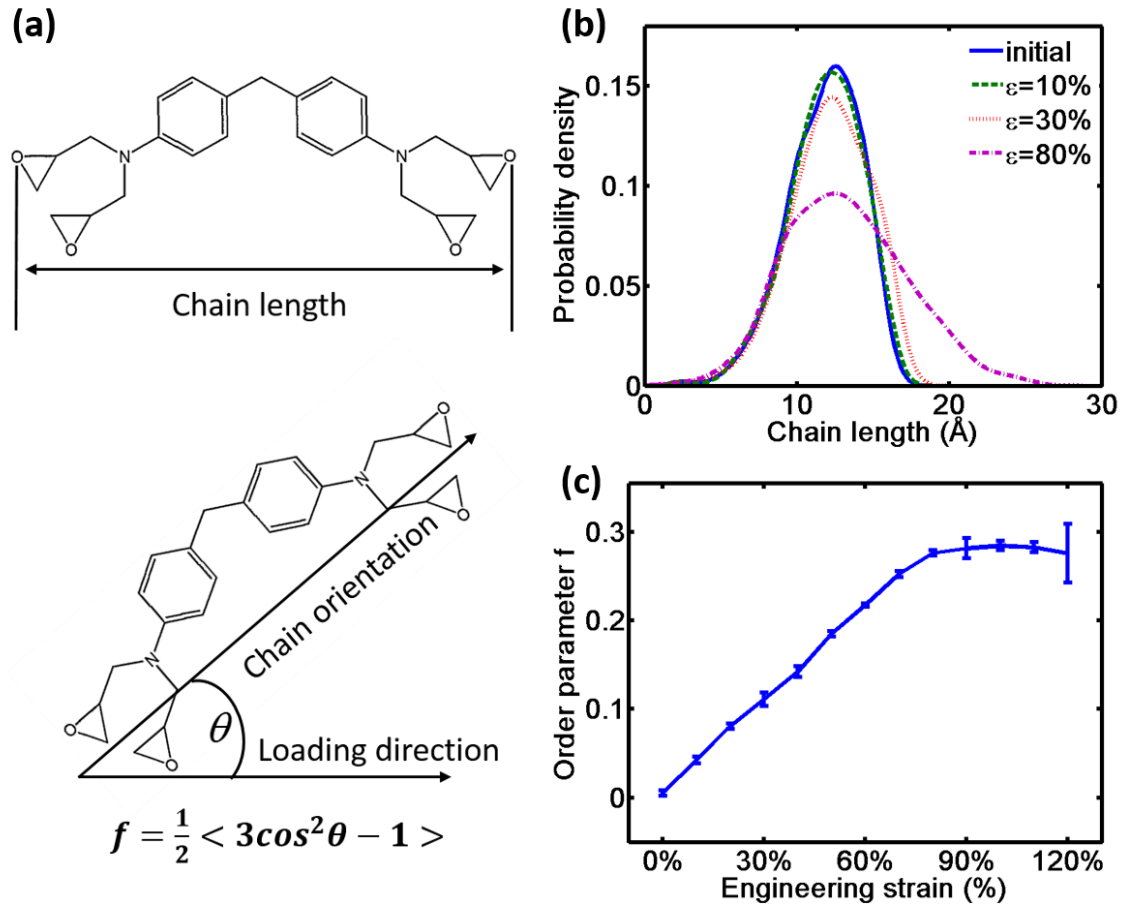

Figure S2. (a) Illustration for definitions of the end-to-end chain length and angle between chain orientation and loading direction for monomer TGMDA in epoxy resin 3501-6. (b) Chain length distribution of monomer TGMDA at different deformation states. (c) Herman's order parameter evolution of monomer TGMDA along deformation.

1.3. Void development

We use Zeo++ software (http://www.maciejharanczyk.info/Zeopp/), which is based on Voronoi cell decomposition, to calculate the void space and its distribution. Specifically, for a given spherical probe, Zeo++ can analyze the void space accessible to this probe and the void

distribution using Monte Carlo sampling approach. We calculate the void distribution across the entire stress strain response using probe size equal to the largest free sphere (Df) at each state, which is the maximum size probe that can travel freely in the channels of the structure, as shown in Fig. S3 (a)(b). Also shown in Fig. S3 (a)(b) is the largest included sphere (Di), indicating the largest void size developed in the structure. Both Di and Df increase along the deformation and reach a plateau near the maximum stress regime. This trend is consistent with a recent study that indicates a steady increase of void size in the strain hardening regime and saturation towards the maximum stress regime.[2]

The void distribution is provided in histogram form, and the mean void diameter (MVD) is calculated by performing numerical integration on the distribution histogram. As shown in Fig. S3 (c)(d), the initial MVD at unstressed state is under 0.5 nm, which represents the initial free volume among segments in the structure. The trend of MVD evolution is similar to the trends of Di and Df. We also observe that the calculated MVD in the failure regime (beyond strain 100% for 3501-6 case) shows large variances and thus is not reliable to represent D in Eq. 2. We use the averaged MVD in the maximum stress regime plateau between the dashed line for the parameter D in Eq. 2.

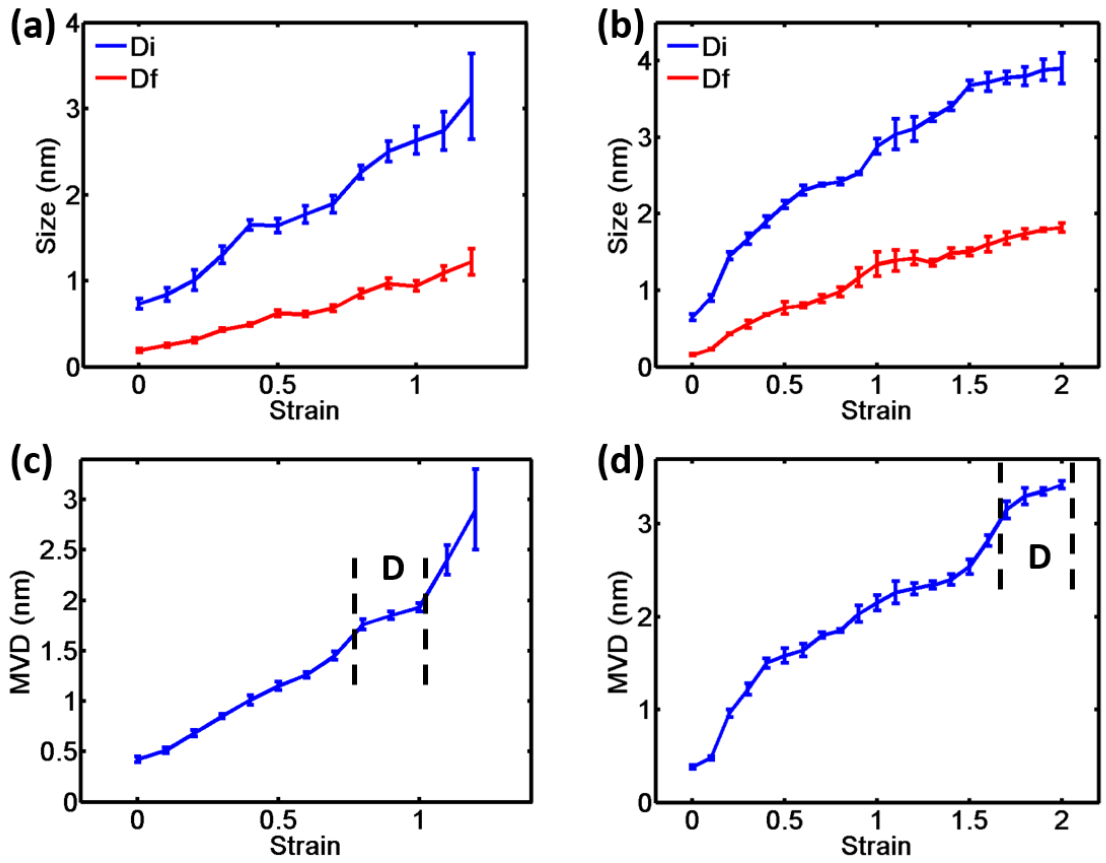

Figure S3. The largest included sphere (Di) and the largest free sphere (Df) evolution during deformation for (a) epoxy 3501-6 and (b) Epon 825. The MVD across the entire stress-strain response of (c) epoxy 3501-6 and (d) Epon 825. The dashed lines show the region where we take the average of MVD to determine the parameter *D* for fracture energy calculation.

1.4. Bond scission

ReaxFF uses distance-dependent bond-order functions to represent the contributions of chemical bonding to the potential energy. The minimum bond-order value used in parameter set ReaxFF_Mattsson to identify chemical bonds between pairs of atoms is set as 0.1. During tensile deformation simulations, the bond information such as total number of bonds can be obtained directly from the ReaxFF implementation. Fig. S4(a) shows the total number of bonds vs. strain for the 3501-6 epoxy resin system at the maximum conversion degree and stoichiometric ratio. We observe that the total number of bonds does not decrease until reaching strain of 75%, which

corresponds to the end of strain hardening regime. This observation also indicates that the scissions of the chains start when the stress approaches its maximum value. After that, the number of bonds decreases steadily. In the final stage, the total number of bonds becomes relatively stable due to the failure of the system (*i.e.* breaking into two parts). This observation is consistent with a recent study using energy based scission algorithm to study the fracture nucleation in cross-linked polymer networks.[2]

In similar way, we calculate the evolution of the number of bonds for epoxy resins of different conversion degrees and compare the number of bonds broken for the different cases as shown in Fig. S4(b). The results show that with increasing conversion degree (*i.e.* increasing crosslink density), the bonds start to break at lower strain, which is consistent with the stress vs. strain curves that show stress maxima at lower strains for greater conversion degrees. In addition, the number of bonds broken after failure increases with greater conversion degree. This can be explained by the greater number of crosslink bonds with increasing conversion degree.

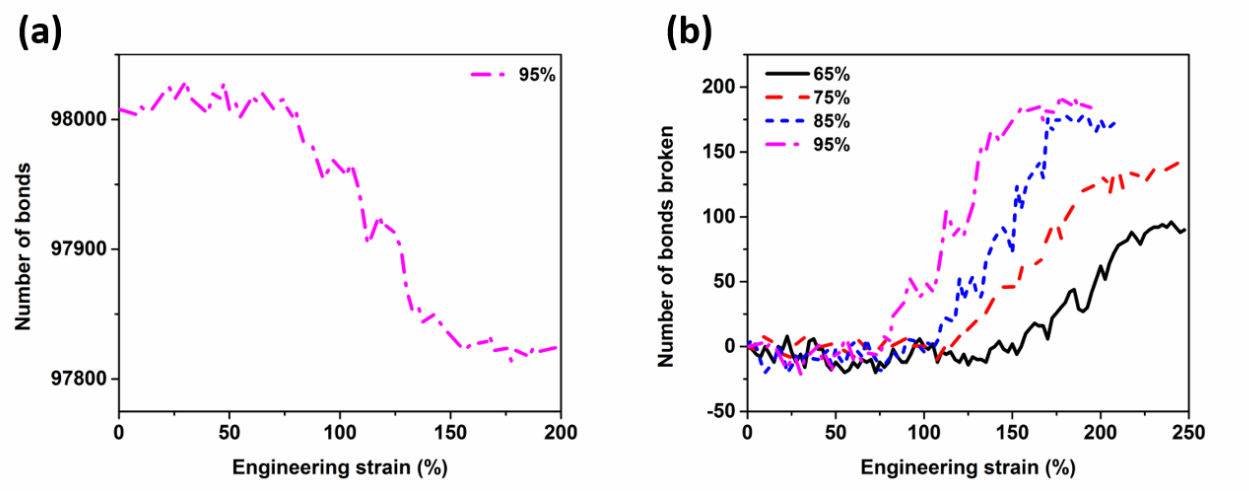

Figure S4. (a). Total number of bonds evolution during deformation for epoxy 3501-6 with maximum conversion degree and stoichiometric ratio. (b). Number of bonds broken during deformation for epoxies 3501-6 with different conversion degrees.

2. Sensitivity analysis for the parameters used to predict fracture energy

In this section, we provide statistical replications of the simulations and justify the variance of the parameters used in Eq. (2) in the main text.

2.1. Statistical replications of the simulations

We first run simulations for the same structure with different initial velocities. Following this, we generate different structures by rerunning the crosslinking process. For non-stoichiometric ratio cases, we also change the ratio between nitrogen atoms that are fully reacted (twice) and those that are partially reacted (once). As a result, the molecular structure can be varied while the overall crosslink density remains the same.

In Fig. S5, it can be observed that the stress-strain curves are very similar for different simulations. There are some statistical variations in the stress-strain curves, which mainly arises from the highly stochastic nature of bond breaking at the failure stage. We quantify the parameters yield stress S and stretch ratio λ from the stress-strain curves by taking the average value over five simulations for each case. The standard deviations of S and λ are within 2% of the average values and the standard deviation of S_{max} is within 5%. Similar standard deviations are also observed for other conversion degree and component ratio cases.

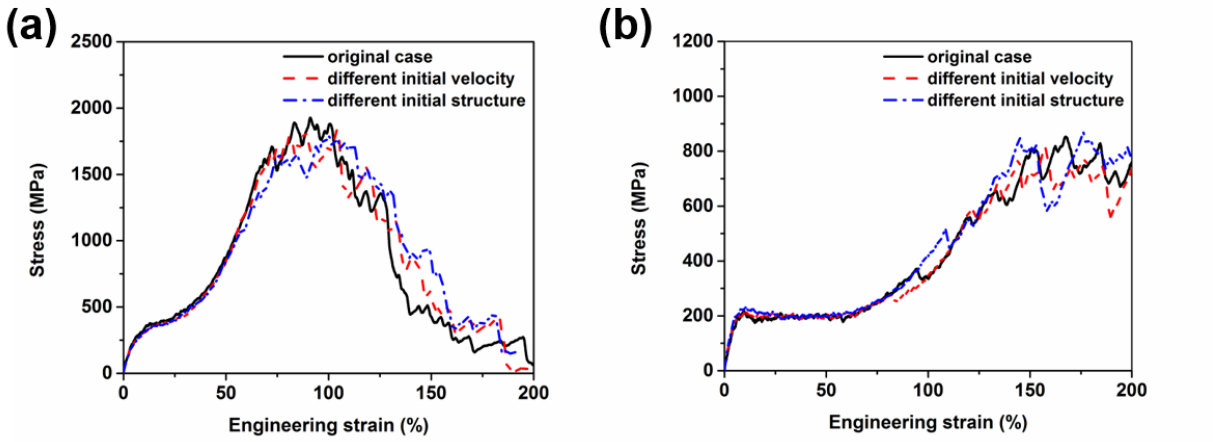

Figure S5. (a). Stress vs. strain curves of multiple simulations for epoxy 3501-6 at stoichiometric ratio and maximum conversion degree. (b). Stress vs. strain curves of multiple simulations for epoxy Epon 825 at stoichiometric ratio and maximum conversion degree.

2.2. Void diameter *D* variances

We state in section 1.3 that we take the average of MVD in the maximum stress regime to determine the parameter *D* for fracture energy calculation. Table S1 lists the MVDs calculated at different strains inside the maximum stress regime indicated in Fig. S3(c) for the 3501-6 case at stoichiometric ratio and maximum conversion degree. The standard deviation of parameter *D* is smaller than 10% of the void sizes and there are no significant differences between different cases, which indicates that the structural deformation always follows a similar cavitation path.

Table S1. Mean Void Diameter (MVD) (nm) for 3501-6 at Stoichiometric Ratio and Maximum Conversion Degree.

	Strain 80%	Strain 90%	Strain 100%	$D \pm$ std
Original case	1.80	1.87	1.89	1.85 ± 0.04
Different velocity	1.74	1.81	1.94	1.83 ± 0.08
Different structure	1.73	1.83	1.97	1.84 ± 0.1

- std is used to abbreviate standard deviation

We also show in Fig. S6 that the calculated void diameter *D* for epoxy resins 3501-6 with different conversion degrees and amine/epoxide ratios, which are used to predict the fracture energies in Fig. 5 of the manuscript. The error bars are introduced due to the range of strains selected and also statistical replications of simulations. We observe an inverse relationship between the void diameter and crosslink density. Specifically, with increasing conversion degree, *i.e.* increasing crosslink density, the void diameter *D* decreases, and the void diameter *D* minimizes for the stoichiometric ratio case (1:1), which has the highest crosslink density.

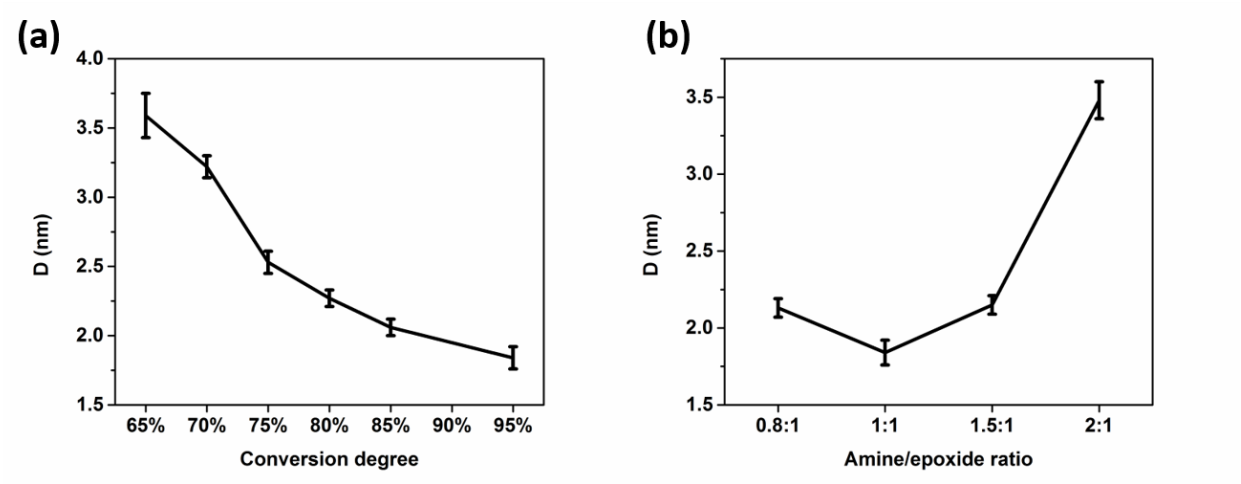

Figure S6. (a) Void diameter D for epoxy resin 3501-6 with different conversion degrees at stoichiometric ratio. (b) Void diameter D for epoxy resin 3501-6 with different amine/epoxide ratios at maximum conversion degrees (>95%).

2.3. Elastic constants calculation

To determine the elastic constants C_{22} and C_{66}, we first equilibrate the deformed structure under NVT ensemble (*i.e.* controlling the deformed shape) at 300K for 20 ps. To obtain C_{22}, we conduct uniaxial tensile deformation in the original stretching deformation while the other two dimensions are fixed. Similarly, to obtain C_{66}, we apply shear deformation to the structure in the 1-2 plane as shown in Fig. 3(a) of the manuscript. In either case, 10% engineering strain is applied to the deformed structure with a constant strain rate of $5 \times 10^8 s^{-1}$. We fit up to 4% strain to get the elastic constants.

To completely quantify the dependence of measured elastic constants on the strain, we calculate the value of $\sqrt{C_{22}/C_{66}}$ at 10% strain increments during deformation, and plot the results in Fig. S7(b). The ratio fluctuates considerably in the failure regime (strain >75%) since the structure becomes unstable due to the chain scission events, as evident from the error bar for the last data point. From these results, we find that the ratio first decreases and then increases, finally reaches a plateau in the strain hardening regime. This plateau also coincides with the constant slope in the strain hardening regime of stress vs. strain curve shown in Fig. S7(a).

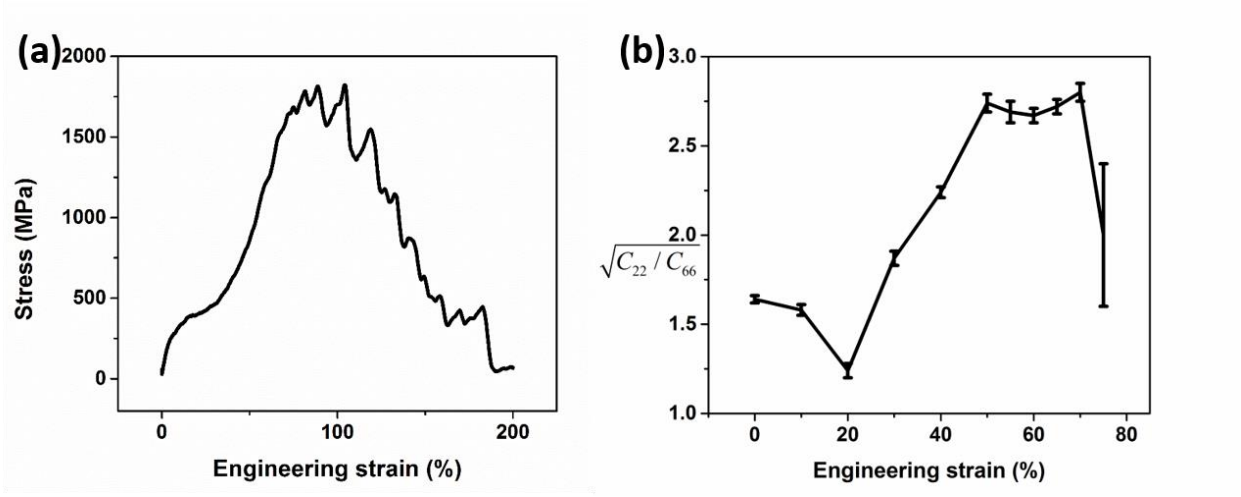

Figure S7. (a) Stress strain curve of epoxy 3501-6 at stoichiometric ratio and maximum conversion degree. (b) $\sqrt{C_{22}/C_{66}}$ calculated before the maximum stress regime of (a).

According to the original model, the elastic constants used in the Eq. (2) are the average elastic constants of the whole process zone.[3, 4] While it is challenging to simulate the whole process zone through MD simulations, we choose the similar route as reported by Rottler *et al.*,[5] in which they used a range of strain states where the stress rises into hardening stage and calculated the elastic constants at different strain levels. Given that the average stress state of the process zone should be between the maximum stress state at the crack tip and the yield stress state at the boundary of the process zone, choosing the average $\sqrt{C_{22}/C_{66}}$ result in the strain hardening stage (strain 50%~70%) also has physical meaning. Therefore, $\sqrt{C_{22}/C_{66}}$ calculated in this study is both physically meaningful and numerically reliable to quantify the anisotropy of the process zone and predict the fracture energy based on Eq. (2).

We also note that the term $\sqrt{C_{22}/C_{66}}$ is a simplified version for the original form:

$$\sqrt{[2(1-A_2)+\left(\frac{C_{22}}{C_{66}}\right)(1-A_1)]/[(1-A_1)^2]}$$

where $A_1 = 2A_2C_{12}/C_{22}$ and $A_2 = C_{12}/(C_{11}+C_{13})$, and $C's$ are the elastic constants, as indicated in Rottler *et al.*'s study.[5] The simplification is validated when the elastic constant in the

stretching direction (C_{22}) is much larger than the others, which are in the same order of magnitude, given that $A_1 \sim 0, A_2 \sim 1$.

Table S2 lists the elastic constants in other directions for 3501-6 epoxy resins and results calculated using both original and simplified form. First, we can observe that the modulus in the stretching direction (C_{22}) is much larger than the moduli in other directions, and the shear modulus (C_{66}) is almost the same as the tensile modulus normal to the stretching direction (C_{11}). The results also justify the accuracy of using the simplified form for epoxy systems, with less than 10% difference between using the simplified and original form. We have also verified that the accuracy holds true for all epoxy chemistries studied here.

Table S2. Elastic constants and results calculated using both original and simplified form for epoxy resin 3501-6 at stoichiometric ratio and maximum conversion degree (the units for the elastic constants are GPa).

	Strain 50%	Strain 55%	Strain 60%
C_{22}	7.5	10.0	12.1
C_{66}	1.0	1.45	1.7
C_{11}	0.9	1.3	1.45
$\sqrt{C_{22}/C_{66}}$	2.74	2.63	2.67
original form	2.96	2.84	2.90

2.4. Stretch ratio λ

Similar to the elastic constants, the stretch ratio λ is associated with the average strain level of the process zone. Higher value of λ indicates higher deformability of the epoxy resin. Although different definitions of stretch ratio would change the value of calculated fracture energy, the fracture energies predicted using Eq. (2) are comparable for different systems if the λ value is defined consistently for all epoxy systems. In addition to the choice of λ as the strain level where the stress equal to $(S + S_{\max})/2$ in the main manuscript, we also use two other definitions of λ to calculate the fracture energy, one is the stretch ratio where stress is equal to $1.5S$, and the other

one is the stretch ratio where stress is equal to $0.8S_{max}$. In Fig. S8, it is shown that the fracture energy exhibits a maximum value within the range of conversion degree considered and it increases with increasing ratio of amine curing agent for different λ, which validates the conclusion in our study.

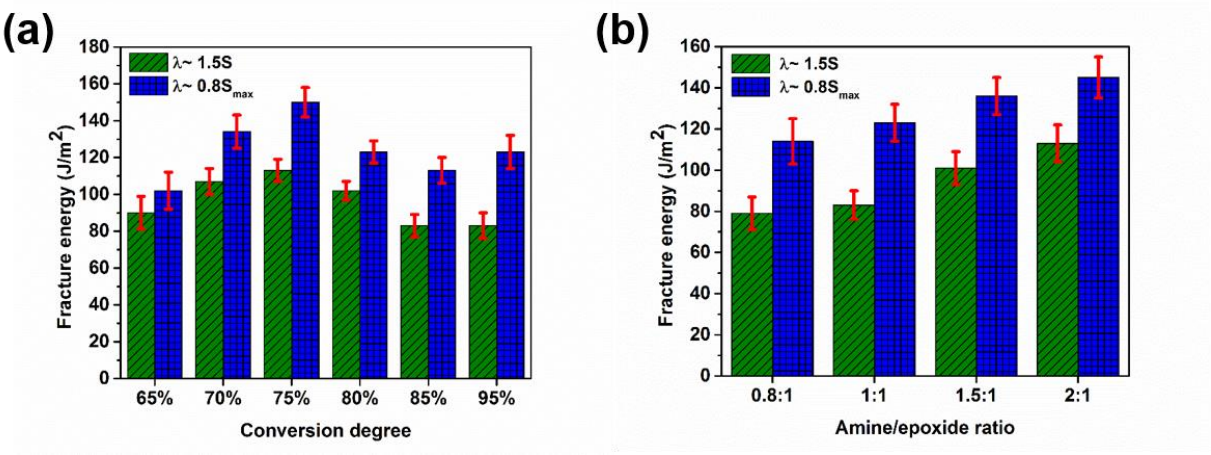

Figure S8. (a). The predicted fracture energy of epoxies with different conversion degrees using two other definitions of λ. (b). The predicted fracture energy of epoxies with different amine/epoxide ratios using two other definitions of λ. The epoxy type is 3501-6.

References

1. Yoshiharu, N.; Shigenori, K.; Masahisa, W.; Takeshi, O. Cellulose Microcrystal Film of High Uniaxial Orientation. *Macromolecules* **1997,** 30, 6395-6397.

2. Moller, J.; Barr, S.; Schultz, E.; Breitzman, T.; Berry, R. Simulation of Fracture Nucleation in Cross-Linked Polymer Networks. *JOM* **2013,** 65, 147-167.

3. Brown, H. A Molecular Interpretation of the Toughness of Glassy Polymers. *Macromolecules* **1991,** 24, 2752-2756.

4. Sha, Y.; Hui, C.; Ruina, A.; Kramer, E. Continuum and Discrete Modeling of Craze Failure at a Crack Tip in a Glassy Polymer. *Macromolecules* **1995,** 28, 2450-2459.

5. Rottler, J.; Barsky, S.; Robbins, M. O. Cracks and Crazes: On Calculating the Macroscopic Fracture Energy of Glassy Polymers from Molecular Simulations. *Phys. Rev. Lett.* **2002,** 89, 148304.